

# Tyrosine side chains as an electrochemical probe of stacked $\beta$ -sheet protein conformations

Anna Loksztajn <sup>a,b</sup>, Wojciech Dzwolak <sup>a,b</sup>, Paweł Krysiński <sup>a,\*</sup>

<sup>a</sup> Faculty of Chemistry, Warsaw University, Pasteura 1, 02-093, Warsaw, Poland

<sup>b</sup> Institute of High Pressure Physics, Polish Academy of Sciences, Sokolowska 29/37, 01-142 Warsaw, Poland

Received 26 February 2007; received in revised form 18 June 2007; accepted 19 July 2007

Available online 27 July 2007

## Abstract

The *in vivo* formation of  $\beta$ -pleated protein aggregates underlies a number of fatal neurodegenerative disorders, such as Alzheimer disease. Since molecular mechanisms of protein misfolding and aggregation remain poorly understood, this has been calling for many diverse biophysical tools capable of addressing different dynamic and conformational aspects of the phenomenon. The two model polypeptides used in this study are poly(L-tyrosine) and insulin. According to FT-IR spectra, poly(L-tyrosine) produced two distinct types of films with dominant either disordered or antiparallel  $\beta$ -sheet conformations depending on carrier solvent used for film's deposition. Electrochemical analysis of both the types of polypeptide films by the means of cyclic voltammetry and differential pulse voltammetry proved that different electrochemical behaviour of the tyrosine residues is determined by the conformation of polypeptide chains. We have rationalized this difference in terms of varying electrochemical accessibility of Tyr residues in each structure.

We have also carried out spectral and electrochemical characterization of insulin  $\beta$ -sheet-rich amyloid fibrils. It appears that the detectable electrochemical response of the protein stems from the presence of four tyrosine residues per insulin monomer. Since hydrophobic residues, among them tyrosines play an important role in the formation of protein amyloid fibrils, but, on a molecular level, may be also critical in explaining neurotoxic properties of aggregates, their electrochemical properties may become a very valuable complementary tool in biophysical studies on protein misfolding.

© 2007 Elsevier B.V. All rights reserved.

**Keywords:** Amyloids; Polyaminoacids; Tyrosine; Electrochemistry; Differential pulse voltammetry

## 1. Introduction

Aggregation and formation of  $\beta$ -pleated fibrils are what often follow when native protein structure is destabilized. The importance of this phenomenon stems from the fact that such  $\beta$ -sheet-rich, non-native protein assemblies (the so-called amyloids) were implicated in the etiology of several degenerative disorders, such as Alzheimer disease [1,2]. Many proteins, even with a marginal sequential propensity to the  $\beta$ -sheet fold (e.g., myoglobin) [3] may acquire the ability to form fibrils under destabilizing conditions. One of the most interesting, yet least understood aspects of protein aggregation, is its polymorphism, which often manifests in a number of distinct (in terms of

morphology, conformation, and biological activity) types of fibrils being formed out of a single amino acid sequence [4]. This problem is particularly important in light of the so-called “prion strains”, when subtle, self-propagating conformational variability is accompanied by dramatic clinical consequences. As it can be rationalized that non-polar amino acids, among them tyrosines, are critical in determining stacking modes associated with particular types of protein fibrils [5], adequate biophysical tools that would address this problem are sought. Electrochemistry is an as yet unexplored approach in this field. Because electrochemical activity of tyrosine is expected to depend strongly on fine topological and nano-environmental features of its surroundings, this has motivated our interest as to whether electrochemistry can provide conformation-sensitive tools for biophysics. Given that burial of non-polar amino acid residues and the ensuing increase in solvent entropy [6] is thought to be

\* Corresponding author. Tel.: +48 22 0211x389; fax: +48 22 8225996.  
E-mail address: [pakrys@chem.uw.edu.pl](mailto:pakrys@chem.uw.edu.pl) (P. Krysiński).

one of the main driving forces of protein aggregation, focusing on electrochemical properties of non-polar, bulky tyrosine aromatic rings can provide a unique insight into the dynamics of aggregating or aggregation-prone protein conformations. This is so because molecular-scale factors affecting electrochemical activity of these residues, such as: solvent-accessibility, local dielectric constant, presence of neighbouring charged residues, or  $\pi-\pi$  interactions with other aromatic moieties are determined by conformation and dynamics of a polypeptide backbone.

We used insulin amyloid as model  $\beta$ -pleated protein fibrils, which are well-characterized structurally, including their strain-like behaviour [7,8]. While the presence of 4 tyrosines per insulin monomer suggests feasibility of electrochemical studies of insulin fibrils, it is necessary to put forward a mechanism of electrochemical activity of the tyrosine residues using a simplified, yet adequate polypeptide model. Poly(L-tyrosine) proves to be an excellent model in this respect.

## 2. Experimental

### 2.1. Samples

Anhydrous LiClO<sub>4</sub> (BDH laboratory reagents), poly-(L-Tyr) (MW 29,700 Da, Sigma), bovine insulin (Sigma), saturated NH<sub>3</sub> aqueous solution (NH<sub>3</sub> aq) (Chempur) and tetrahydrofuran (THF, Sigma) were used without further purification. All solutions were prepared using deionised water (from Q-Millipore). Insulin amyloid was obtained through a 48 h incubation of 1 wt.% native protein in 0.1 M NaCl, pH 1.9 at 60 °C (pH was adjusted using solution of DCl in D<sub>2</sub>O for the case of FTIR experiments or HCl and H<sub>2</sub>O for electrochemical ones), pH adjustment was controlled using pH-meter. The D<sub>2</sub>O environment enabled acquisition of protein FTIR spectra in the transmission mode. Poly(L-tyrosine) films were obtained by dropping a diluted solution of the polypeptide (either in NH<sub>3</sub> aq or THF) onto a substrate surface (CaF<sub>2</sub> window for FT-IR, and GCE working electrode for electrochemical measurements) and leaving it to dry up at room temperature. After the acquisition of dry film spectra, the same sample was covered with deuterated electrolyte solution, tight-covered with a second CaF<sub>2</sub> window and FTIR spectra in the transmission mode were recorded again.

### 2.2. Electrochemistry/FTIR spectroscopy

Electrochemical measurements were performed with an AUTOLAB analyzer (ECO CHEMIE, Switzerland). A standard cell with three-electrode system was used. A glassy carbon electrode (GCE, Bioanalytical Systems, and Inc.BASI, USA) was used as a working electrode. Prior to each measurement the GCE electrode (0.07 cm<sup>2</sup> geometric area, Bioanalytical Systems, Inc., USA) was polished with 0.05 µm grade Al<sub>2</sub>O<sub>3</sub> slurry and washed thoroughly in deionised water. For all experiments, an Ag/AgCl/1MKCl<sub>aq</sub> electrode was used as the reference electrode, while platinum wire was used as the counter electrode. All experiments were carried out at 25 °C in deaerated solutions. Electrochemical measurements were conducted at pH 2–7. Within this range of pH neither poly(L-tyrosine) nor amyloid

films are soluble, which allowed for an electrochemical characterization of the solid film deposits of the polypeptide and the protein.

Infrared spectra were collected on a Nicolet NEXUS FT-IR spectrometer. For each spectrum, 256 interferograms of 2 cm<sup>-1</sup> resolution were co-added. For data processing, GRAMS (ThermoNicolet) was used.

## 3. Results and discussion

Poly(L-tyrosine) was chosen as the simplest tyrosine-rich polypeptide capable of formation of  $\beta$ -pleated conformation, a property shared with other protein aggregates and amyloid fibrils in particular. A number of polymerized amino acids (e.g. polylysine) are capable of adopting distinct secondary folds depending on conditions of pH, temperature and the presence of non-polar co-solvents [6,9]. These effects can be rationalized in terms of repulsive interactions between charged side chains (i.e. only within the charge-depleting pH range an ordered structure is allowed), and compensation of the cost of decreasing configurational entropy of orderly-stacked chains with the increasing overall solvent entropy [6]. We have taken advantage of these effects to create two distinct backbone conformations of poly(L-tyrosine) and compare their electrochemical behaviour.

Fig. 1 shows FTIR spectra of poly(L-tyrosine) dry films formed through solvent evaporation from saturated solutions of the polypeptide in NH<sub>3</sub> aq (Fig. 1A, solid line) and THF (Fig. 1B, solid line). Fig. 1C shows spectra of native (dashed line) and aggregated insulin (insulin amyloid, solid line). Subsequently, the same polypeptide films were measured after immersion in deuterated electrolyte solution (Fig. 1A and B, dashed lines). The reason for the FTIR experiments in deuterated solution will be discussed below.

The conformation-sensitive amide I band visible between 1600 and 1700 cm<sup>-1</sup> undergoes the characteristic splitting when NH<sub>3</sub> aq has been used as the solvent in poly(L-tyrosine) films preparation. The presence of the two bands: major at 1632 cm<sup>-1</sup> and minor at 1695 cm<sup>-1</sup> (in an undeuterated protein) points to an antiparallel  $\beta$ -sheet as the basic secondary component of the polypeptide film [6]. If NH<sub>3</sub> aq is replaced with THF for the film preparation, the amide I band reveals quite different characteristics: a broad peak centered at 1655 cm<sup>-1</sup> which should be attributed to unordered conformations with a likely overlap from some helical structures. The spectra show a number of other bands that are less diagnostically useful, and are attributed to tyrosine aromatic rings [10]. Fig. 1 shows also the difference between the native and aggregated insulin spectra. The band at 1649 cm<sup>-1</sup> (dashed line) is characteristic for  $\alpha$ -helical conformation of native protein, while the band around 1628 cm<sup>-1</sup> (solid line) reflects the presence of the parallel  $\beta$ -sheet: the dominant secondary structure in the aggregated insulin. The data in Fig. 1A and B show how the conformation of poly(L-tyrosine) in the films can be controlled by the “history of solvation” rather than by any chemical modifications, which allows (once the films are dried) to carry out a comparative electrochemical characterization of both conformations under an identical set of physicochemical conditions. In unison to the FTIR results, the electrochemical behaviour

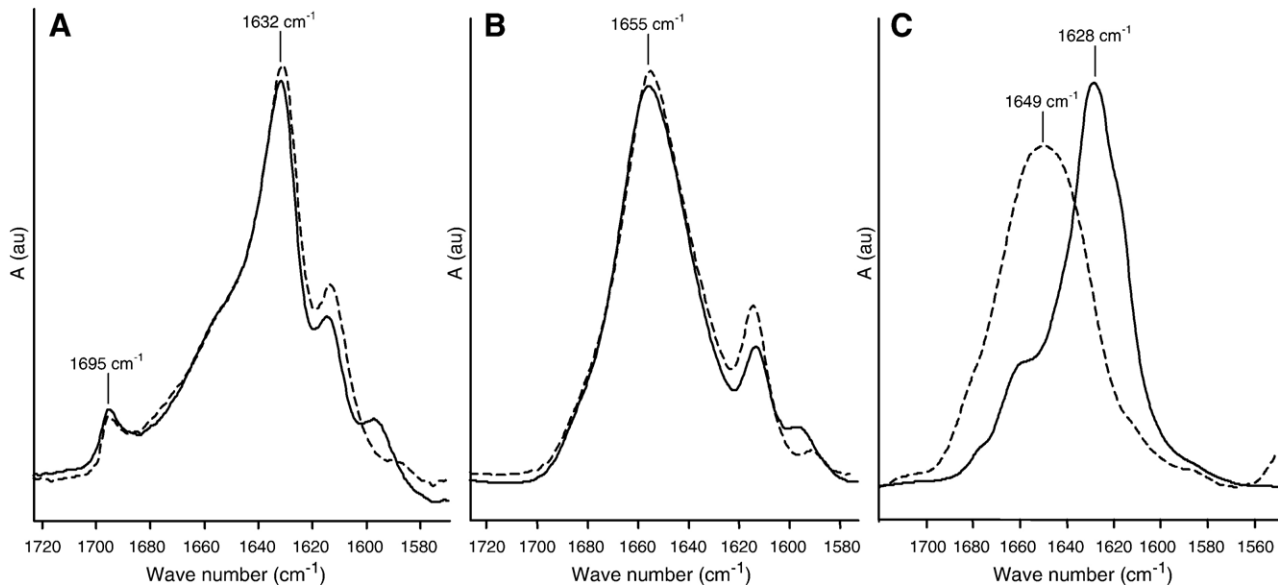


Fig. 1. (A) FTIR spectra of undeuterated poly(L-tyrosine) film obtained from  $\text{NH}_3$  aq ( $\beta$ -sheet structure; solid line) and the same film in deuterated electrolyte solution (dashed line); (B) FTIR spectra of undeuterated poly(L-tyrosine) film obtained from THF (random coil structure; solid line) and the same film in deuterated electrolyte solution (dashed line); (C) FTIR spectra of deuterated native (dashed line) and deuterated aggregated insulin (solid line).

of films deposited on GCE depends on the solution from which they were formed. In order to eliminate a possible effect of electrolyte solution re-wetting the films, the FTIR spectra of the same polypeptide films were measured after their immersion in deuterated electrolyte solution (Fig. 1A and B, dashed lines). There are no changes in spectral characteristics and therefore in secondary structure of dry films of poly(L-tyrosine) after their immersion in the electrolyte solution. Since the duration of FTIR acquisition was comparable to the electrochemical experiments, we can rationalize that the observed behaviour described below, is due solely to the electrooxidation of these films. The differential pulse voltammetry (DPV) technique shows significant difference between poly(L-tyrosine) films (Fig. 2). Measurements were carried out in 0.01 M  $\text{HClO}_4$ , 0.1 M  $\text{LiClO}_4$  solution.

First, it is evident that the films deposited from  $\text{NH}_3$  aq are oxidized at less positive potentials (at ca. 850 mV, Fig. 2A) as compared to the films deposited from THF (at ca. 1050 mV, Fig. 2B). Since DPV is a differential technique, the current/voltage response of the system under study corresponds to the first derivative of a conventional voltammogram, with the peak potential approximately identifiable with the half-way potential. Having said that, it is evident that ca. 20 kJ/mol per electron transfer less free energy is required to oxidize the same polypeptide in a film deposited from a hydrophilic solvent as compared with the hydrophobic one. We believe that this may result from different electrochemical accessibility of Tyr residues in well-ordered,  $\beta$ -pleated films obtained from  $\text{NH}_3$  aq as compared to random coil structures obtained from THF solutions. Moreover, the subsequent scan reveals a decrease of these peaks in both systems, while for the case of poly(L-tyrosine) films from  $\text{NH}_3$  aq a new peak appears at ca. 410 mV on the oxidation scan. This feature is not observed for the films from THF.

It appears that depending on solvents used for dry films deposition, the electrooxidation products of poly(L-tyrosine)

vary. One might question however, whether the observed behaviour is not determined by the interactions between the polypeptide and the electrode surface, and not by the structural conformations in the “bulk” of the deposited films. Obviously, we could not eliminate such interactions, yet the glassy carbon and carbon-based electrodes are widely used as an “inert” electrode in terms of peptide electrochemistry [11–14,21–23]. To the contrary, the use of gold electrode in our experiments yielded only one type of voltammetric curve for the systems studied (as in Fig. 2A), regardless of the solvent from which the films were formed (data not shown).

In order to assign the characteristic features observed on these two voltammograms to particular redox processes, we have conducted a series of cyclic voltammograms of insulin amyloid, poly(L-tyrosine) film (from  $\text{NH}_3$  aq solution) and L-tyrosine, all in 0.01 M  $\text{HClO}_4$ , 0.1 M  $\text{LiClO}_4$  aqueous solutions,  $\text{pH}=2$  (Fig. 3).

Cyclic voltammetry upon the first anodic scan produced a poorly developed peak characteristic for the Tyr oxidation ( $\sim 950$  mV) [11–14]. Even though Fig. 3 shows that cyclic voltammetry is not the technique of choice for this case, it reveals some interesting behaviour of the studied systems. In the case of amyloid and poly(L-tyrosine) films the oxidation peaks appear at roughly the same position. In all three cases, subsequent scans resulted in the decrease of these peaks. A closer inspection of the cyclic voltammograms reveals that while for the L-tyrosine film no additional peaks are found upon the reverse scan and continuous cycling, both the amyloid film (Fig. 3A) and poly(L-tyrosine) film (Fig. 3B) show a pair of peaks centered around 350 mV. The peak on the cathodic branch (at ca. 250 mV) appears immediately upon return from the first anodic scan if reversed at 1100–1200 mV. It will not appear if CV scan is reversed at the threshold of the anodic peak (ca. 800 mV). The same holds true for the anodic peak at ca. 460 mV. Since such a behaviour is not observed for the case of L-tyrosine film (Fig. 3C), it is

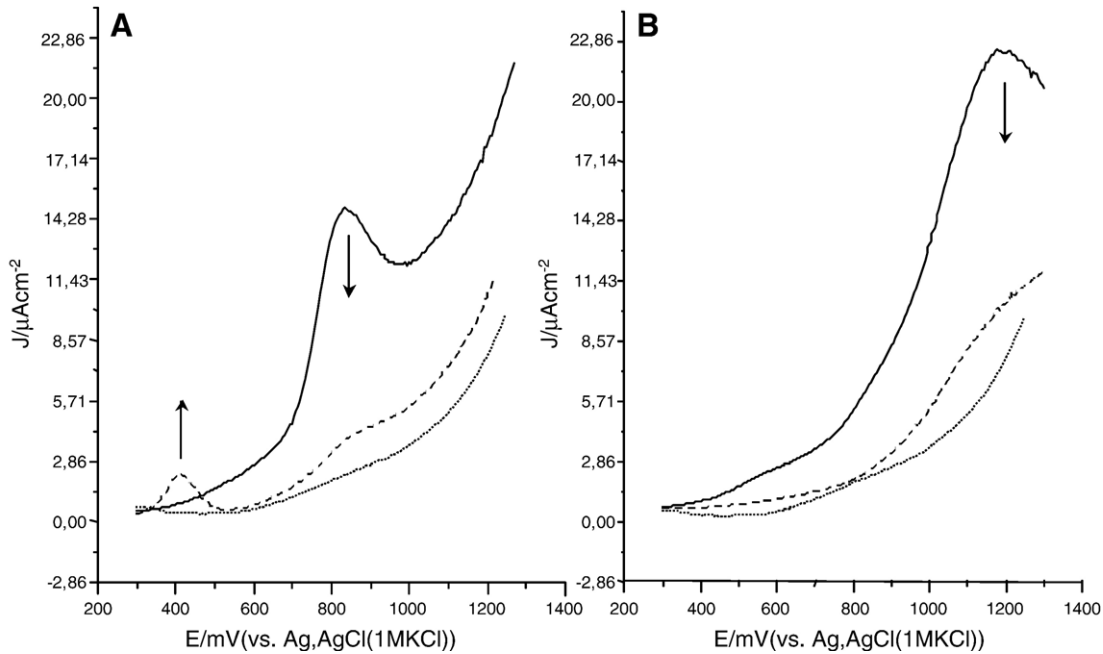


Fig. 2. Differential pulse voltammograms of poly(L-tyrosine) films formed through solvent evaporation from saturated solutions of the polypeptide in  $\text{NH}_3$  aq (A) and THF (B) in 0.01 M  $\text{HClO}_4$ /0.1 M  $\text{LiClO}_4$  electrolyte ( $\text{pH}=2$ ). First (solid line) and fifth (dashed line) scans of each measurement are shown. Bare GCE electrode in the same solution — dotted line. To avoid residual solvents affecting the electrochemical response, the “bare” electrode was treated with either  $\text{NH}_3$  aq or THF solution and allowed to dry in air before the experiments.

evident that the oxidation products of Tyr residues in insulin or poly(L-tyrosine) films are different from those obtained for “free” tyrosine molecules.

Because poorly developed characteristics discussed above are difficult to test (particularly for the case of the amyloid films with only 4 Tyr units per insulin molecule), we decided to use the differential pulse voltammetry (DPV) technique that allows for a better resolution of voltammetric peaks, which proved advantageous in earlier protein [15] and amyloid studies [16]. Particularly, the studies by Vestergaard et al. [16] on the electrochemical detection, characterization and kinetics of the

aggregation of Alzheimer’s disease amyloid  $\beta$  peptides (A $\beta$ -40 and A $\beta$ -42) proved the usefulness of DPV technique for such experiments. These studies are of particular relevance to the present work, since the aggregation kinetics was monitored via the oxidation of Tyr residues of the amyloid peptides.

Fig. 4 shows that in accordance to the cyclic voltammetry experiments, the electrochemical responses of amyloid (Fig. 4A) and poly(L-tyrosine) (Fig. 4B) show a similar behaviour in terms of the anodic peak at 410 mV (this peak corresponds to the 460 mV peak in cyclic voltammetry technique). And, as expected, no peak is detected for the “free” Tyr system (Fig. 4C). The same

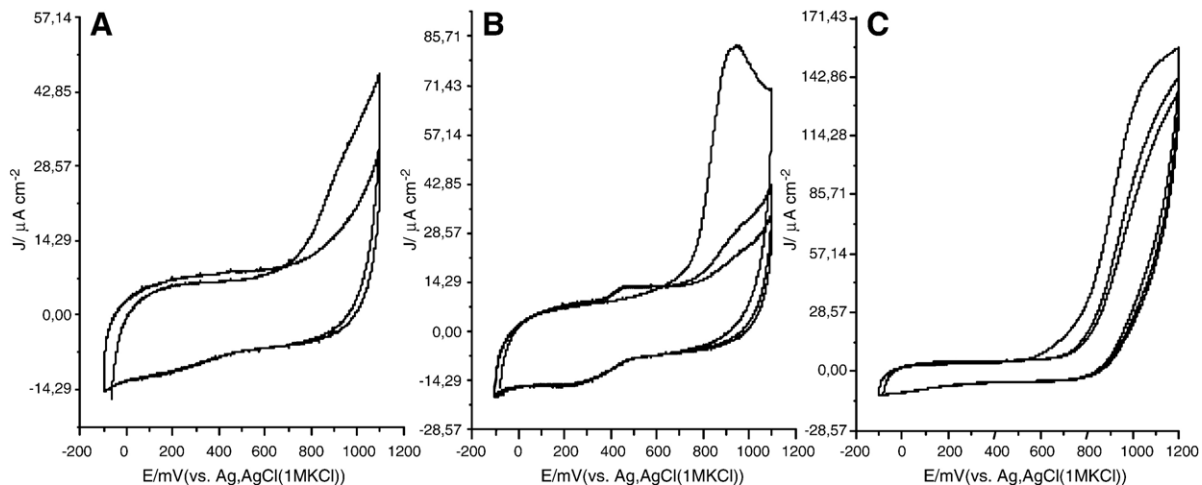


Fig. 3. Cyclic voltammograms of: insulin amyloid film (A), poly(L-tyrosine) film (B) and monomeric tyrosine (C). Films were formed through solvent evaporation from  $\text{NH}_3$  aq solution. Measurements were done in 0.01 M  $\text{HClO}_4$ /0.1 M  $\text{LiClO}_4$  electrolyte ( $\text{pH}=2$ ). Three cycles were done in each measurement at 50 mV/s scan rate.

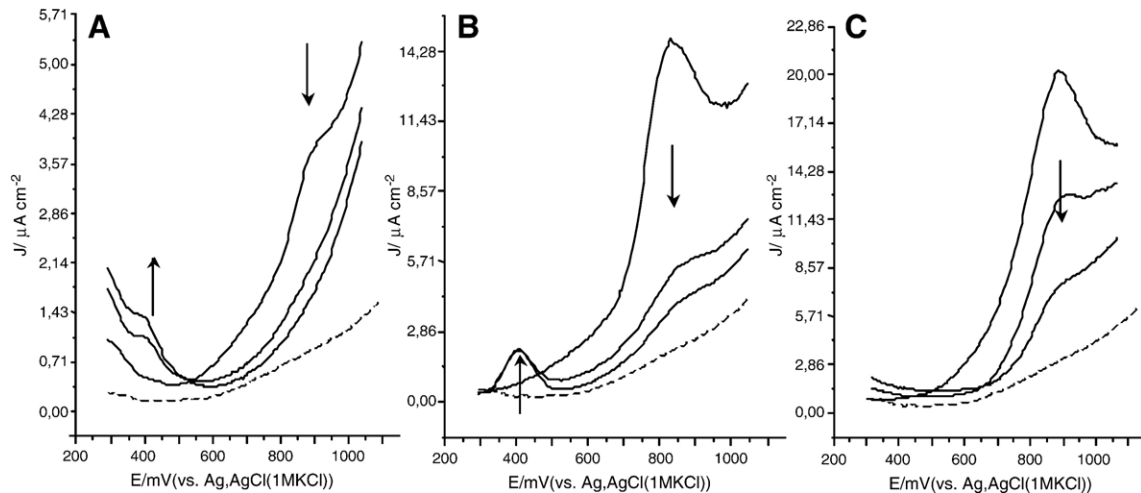


Fig. 4. Differential pulse voltammograms of: insulin amyloid (A), poly(L-tyrosine) (B) and monomeric tyrosine (C). Films were formed through solvent evaporation from  $\text{NH}_3\text{ aq}$  solutions. Measurements were done in 0.01 M  $\text{HClO}_4$ /0.1 M  $\text{LiClO}_4$  electrolyte (pH=2). Five scans were done for each film (first, third and fifth scan are shown). Bare electrode in the same electrolyte solution — dotted line. To avoid residual solvents affecting the electrochemical response, the “bare” electrode was treated with either  $\text{NH}_3\text{ aq}$  or THF solution and allowed to dry in air before the experiments.

CV and DPV measurements were done for native insulin in electrolyte (0.01 M  $\text{HClO}_4$ , 0.1 M  $\text{LiClO}_4$ ) solution (data not shown) and results were analogous to those obtained for the amyloid. Similar results were obtained by Brabec [14] for native insulin.

There exists a vast literature concerning the quite complex oxidation process of tyrosine in solution under similar conditions (electrode material, pH range) as we used. According to the literature data, the major irreversible oxidation peak that appears in all the cases studied in this work at the most positive potentials is connected with radical formation and its position is pH dependent [11–14,17]. This electrooxidation of dissolved L-tyrosine is followed by a chemical step — decarboxylation and then deamination leading to lower aldehyde [18–20], both products being non-electroactive in the potential range studied. Other data suggest the possibility of polymerization [21] as well as formation of cyclohexadienol derivative [21,22] or quinone-type products [19,22,23]. For all of those studies carbon electrodes were used (mostly GCE) and measurements were done for the similar pH range. In our view the chemical steps involving decarboxylation and deamination can be excluded, since both functionalities are involved in the formation of peptide chains in the amyloid as well as poly-L-Tyr films. This fact, along with the appearance of the pair of CV peaks centered around 350 mV solely for the amyloid and poly-L-Tyr films, points towards the reaction path leading to the quinone-type products. Such a pathway that involves hydroxylation leading to quinone derivatives has already been reported for electro-oxidation of tyramine [23] as well as for the enzymatic hydroxylation of tyrosine [24] both processes leading to the catechol, DOPA or dopamine. What is most important is that those results [23,24] were also obtained for carbon electrodes in the same pH range as we used in the present work. These reactions, though of small yield (ca. 10%), resulted in the appearance of voltammetric peaks characteristic for the quinone/hydroquinone redox pair and centered on ca. 410 mV

for pH 2. Comparing the amount of charge under the oxidation peak at +0.9 V with that above 0.41 V in the cyclic voltammetry experiments shows indeed that only a very small part of the oxidation product formed above +0.9 V is converted into the electroactive pair [23], the other products remain unknown. Therefore, we believe that the final electrooxidation product of amyloid film as well as poly-L-Tyr film deposited on GCE electrode from  $\text{NH}_3\text{ aq}$  is an *o*-quinone-type product, giving the pair of redox peaks centered around 410 mV at pH 2. Our preliminary conclusions are supported also by spectral data of Ogura et al. [20] who studied the electrochemical oxidation of free L-tyrosine. By means of in-situ FTIR they have concluded that one of the products of amino acid electrooxidation is phenol. The same product was detected by Zinola et al. [19] who also found a complex signal at  $1650\text{--}1675\text{ cm}^{-1}$  that originated from the vibration of the carbonyl group of a benzoquinone.

We have tested also the dependence of observed DPV oxidation peaks on pH. The anodic peak at 0.90 V as well as the

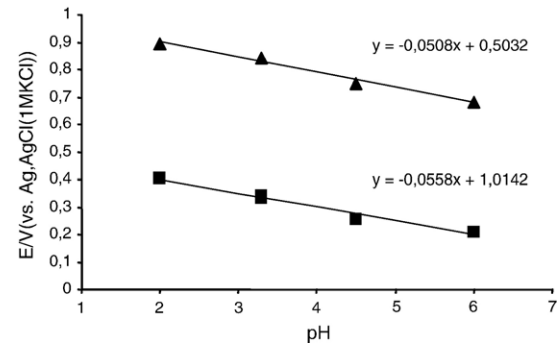
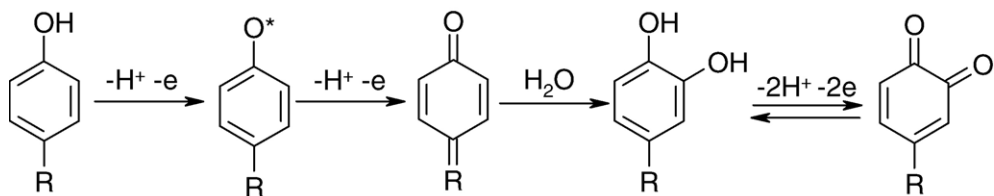


Fig. 5. pH dependence of tyrosine oxidation peak (triangles) and quinone-type product of tyrosine oxidation (squares) corresponding to  $E^{\max}$  of DPV peak. Measurements were done in appropriate mixture of 0.01 M  $\text{HClO}_4$  and 0.1 M  $\text{LiClO}_4$  for pH adjustment, keeping the ionic strength constant.



Scheme 1. Proposed mechanism of electrooxidation of tyrosine in polypeptide and protein involving diol formation and *ortho*-quinone as a final product of reaction on electrode.

pair of peaks around 0.41 V should be pH dependent [25,26]. As shown in Fig. 5, both peaks exhibit similar linear dependencies of their position on pH. The slopes of these dependencies are close to 59 mV per unit pH, therefore characteristic for the number of electrons to protons ratio ( $e/H^+$ ) equal to one for both redox processes. The position of DPV oxidation peak, that is characteristic for Tyr (as well as other phenol derivatives) oxidation (Fig. 5, triangles), changes from 900 mV (pH=2) to 700 mV (pH=6). Linearity of this characteristics with slope equal to 51 mV seems to be in agreement with  $H^+/e$  ratio close to unity for the oxidation process. This behaviour is well known and described [11–14,27].

The position of DPV peak connected with the redox couple (Fig. 5, squares) changes linearly with the characteristic slope of 56 mV per unit pH. This result is similar to that obtained for dopamine [26], L-DOPA [28] and adrenaline [29]; in all cases the final product was a quinone derivative.

Based on these results we propose the following preliminary mechanism for Tyr oxidation, which is supposed to be the same for both the amyloid and model poly-L-Tyr polypeptide chains (Scheme 1).

The first stage of oxidation is the formation of phenoxyradical, which is a typical and well described mechanism for electrooxidation of phenolic compounds [30–33]. The next step is chemical reaction — the hydroxylation process leading to the formation of a diol. The last step is the quasi-reversible electrooxidation of this diol to *ortho*-quinone. The first and the last steps are responsible for the electrochemical signals at ca. 900 mV and 410 mV, respectively, at pH=2 electrolyte. We are aware that this scheme accounting for our results is a preliminary one that is worth of detailed experimental elaboration in our future work.

Similar interpretation of the reaction route was presented by Longchamp et al. [34] to explain electrochemical properties of plasmin adsorbed onto a carbon paste electrode. This protein contains both the tyrosine and tryptophan residues and it was suggested that upon oxidation these groups form quinone derivatives on the electrode surface. Yet another example of similar reaction pathway is the electrochemical oxidation of neurotransmitter serotonin. 5-Hydroxytryptamine (serotonin) is a phenolic derivative and similar to tyrosine, the *para* position in its ring is inactive for electrooxidation [35,36]. Moreover the oxidation of Tyr to dopaquinone and then to other products occurs in living organisms. Under physiological conditions these two steps are enzymatically catalyzed by tyrosinase [37]. For example this reaction is involved in biosynthesis of melanin [38].

Electrochemical oxidizability of proteins can be exploited for the investigation of the accessibility of tyrosine residues in protein molecules for interaction with their environment (what was suggested earlier by Brabec [14]). It seems to be very important and can be useful especially in analysis of amyloid fibril structure since amino acid configuration inside and outside fibril remains unknown.

#### 4. Conclusions

Poly(L-tyrosine) was used as a model for electrooxidation of insulin amyloid. By means of FTIR experiments, two morphologically distinct secondary structures were shown for this polyaminoacid that depend only on the hydrophilicity and transient pH of the solution from which the films were formed (“history of solvation”). One of these structures –  $\beta$ -sheet – is the common structure motif in both poly(L-tyrosine) deposited from  $\text{NH}_3$  aq and insulin amyloid. Electrooxidation of tyrosine residues in these species was followed on a glassy carbon electrode. It was also shown that the electrooxidation pathway depends upon the type of the solvent from which the polypeptide films were deposited on the electrode surface. Similarities in the electrochemical behaviour of insulin amyloid and poly(L-Tyr) film that was deposited from  $\text{NH}_3$  aq were interpreted in terms of similar,  $\beta$ -pleated structures formed in the peptide. This was supported by FTIR experiments. The spectrum of poly(L-Tyr) films deposited from THF showed no such structures and their electrochemical behaviour differs as well. We explain these observations in terms of better electrochemical accessibility of Tyr residues in well-ordered,  $\beta$ -pleated films as compared to random coil structures obtained from THF solution. Thus, poly(L-tyrosine) is a good model for analysis of insulin amyloid behaviour on the electrodes.

#### Acknowledgment

We are grateful to the Ministry of Scientific Research and Information Technology for support through Project No. PBZ 18-KBN-098/T09/2003 for the years 2004–2007.

#### References

- [1] C.M. Dobson, Protein folding and misfolding, *Nature* 426 (2003) 884–890.
- [2] V.N. Uversky, A.L. Fink, Conformational constraints for amyloid fibrillation: the importance of being unfolded, *Biochim. Biophys. Acta* 1698 (2004) 131–153.

[3] M. Fandrich, M.A. Fletcher, C.M. Dobson, Amyloid fibrils from muscle myoglobin, *Nature* 410 (2001) 165–166.

[4] P. Chien, J.S. Weissman, A.H. DePace, Emerging principles of conformation-based prion inheritance, *Annu. Rev. Biochem.* 73 (2004) 617–656.

[5] W. Dzwolak, S. Grudzielanek, V. Smirnovas, R. Ravindra, C. Nicolini, R. Jansen, A. Lokszejn, S. Porowski, R. Winter, Ethanol-perturbed amyloidogenic self-assembly of insulin: looking for origins of amyloid strains, *Biochemistry* 44 (2005) 8948–8958.

[6] W. Dzwolak, R. Ravindra, C. Nicolini, R. Jansen, R.J. Winter, The diastereomeric assembly of polylysine is the low-volume pathway for preferential formation of  $\beta$ -sheet aggregates, *J. Am. Chem. Soc.* 126 (2004) 3762–3768.

[7] R. Jansen, W. Dzwolak, R. Winter, Amyloidogenic self-assembly of insulin aggregates probed by high resolution atomic force microscopy, *Biophys. J.* 88 (2005) 1344–1353.

[8] W. Dzwolak, V. Smirnovas, R. Jansen, R. Winter, Insulin forms amyloid in a strain-dependent manner: an FTIR spectroscopy study, *Prot. Sci.* 13 (2004) 1927–1932.

[9] D. Carrier, H.H. Mantsch, P.T.T. Wong, Protective effect of lipid surfaces against pressure-induced conformational changes of poly(L-lysine), *Biochemistry* 29 (1990) 254–258.

[10] A. Barth, The infrared absorption of amino acid side chains, *Prog. Biophys. Mol. Biol.* 74 (2000) 141–173.

[11] J. Guang-Ping, L. Xiang-Qin, The electrochemical behavior and amperometric determination of tyrosine and tryptophan at a glassy carbon electrode modified with butyrylcholine, *Electrochem. Commun.* 6 (2004) 454–460.

[12] A.J. Harriman, Further comments on the redox potentials of tryptophan and tyrosine, *J. Phys. Chem.* 91 (1987) 6102–6104.

[13] R. Stingele, D.A. Wilson, R.J. Traystman, D.F. Hanley, Tyrosine confounds oxidative electrochemical detection of nitric oxide, *Am. J. Physiol.* 274 (1998) 1698–1704.

[14] V. Brabec, Electrochemical oxidation of nucleic acids and proteins at graphite electrode. Qualitative aspects, *Bioelectrochem. Bioenerg.* 7 (1980) 69–82.

[15] X. Cai, G. Rivas, P. Farias, H. Shiraishi, J. Wang, E. Palecek, Potentiometric stripping analysis of bioactive peptides at carbon electrodes down to subnanomolar concentrations, *Anal. Chim. Acta* 332 (1996) 49–57.

[16] M. Vestergaard, K. Kerman, M. Saito, N. Nagatani, Y. Takamura, E. Tamiya, A rapid label-free electrochemical detection and kinetic study of Alzheimer's amyloid beta aggregation, *J. Am. Chem. Soc.* 127 (2005) 11892–11893.

[17] A. Sanchez Perez, F.J. Lucena Conde, Polarographic determination of phenylalanine, tyrosine, methionine, glutamic acid and histidine with a dropping copper amalgam electrode, *J. Electroanal. Chem.* 74 (1976) 339–346.

[18] S.M. MacDonald, S.G. Roscoe, Electrochemical oxidation reactions of tyrosine, tryptophan and related dipeptides, *Electrochim. Acta* 42 (1997) 1189–1200.

[19] C.F. Zinola, J.L. Rodrigues, M.C. Arevalo, E.J. Pastor, FTIR studies of tyrosine oxidation at polycrystalline Pt and Pt(111) electrodes, *J. Electroanal. Chem.* 585 (2005) 230–239.

[20] K. Ogura, M. Kobayashi, M. Nakayama, Y.J. Miho, In-situ FTIR studies on the electrochemical oxidation of histidine and tyrosine, *J. Electroanal. Chem.* 463 (1999) 218–223.

[21] B. Malfoy, J.A. Reynaud, Electrochemical investigations of amino acids at solid electrodes. Part II: amino acids containing no sulfur atoms: tryptophan, tyrosine, histidine and derivatives, *J. Electroanal. Chem.* 114 (1980) 213–223.

[22] J.A. Reynaud, B. Malfoy, A. Bere, The electrochemical oxidation of three proteins: RNAase A, bovine serum albumine and concanavalin A at solid electrodes, *Bioelectrochem. Bioenerg.* 7 (1980) 595–606.

[23] L. Papouchado, G. Petrie, R.N. Adams, Anodic oxidation pathways of phenolic compounds. Part I: anodic hydroxylation reactions, *Electroanal. Chem. Interfac. Chem.* 38 (1972) 389–395.

[24] G.A. Rivas, V.M. Solis, Indirect electrochemical determination of L-tyrosine using mushroom tyrosinase in solution, *Anal. Chem.* 63 (1991) 2762–2765.

[25] A. Afkhami, D. Nematollahi, L. Khalafli, M. Rafiee, Kinetic study of the oxidation of some catecholamines by digital simulation of cyclic voltammograms, *Int. J. Chem. Kinet.* 37 (2005) 17–24.

[26] R. Luz, F.Z. Damas, A. Oliveira, J. Beck, L.T. Kubota, Development of a sensor based on tetracyanoethylenide (LiTCNE)/poly-L-lysine (FILL) for dopamine determination, *Electrochim. Acta* 50 (2005) 2675–2683.

[27] N.C. Reynolds, B.M. Kissela, L.H. Fleming, The voltammetry of neuropeptides containing L-tyrosine, *Electroanalysis* 7 (1995) 1177–1181.

[28] X. Liu, Z. Zhang, G. Cheng, S. Dong, Spectroelectrochemical and voltammetric studies of L-DOPA, *Electroanalysis* 15 (2003) 103–107.

[29] M.D. Hawley, S.V. Tatawawadi, S. PiekarSKI, R.N. Adams, Electrochemical studies of the oxidation pathways of catecholamines, *J. Am. Chem. Soc.* 89 (1967) 447–450.

[30] G.W. Morrow, Anodic oxidation of oxygen-containing compounds, in: M. Lund, O. Hammerich (Eds.), *Organic Electrochemistry*, 4th ed., Marcel Dekker, New York, 2002, pp. 589–618.

[31] M.S. Ureta-Zanartu, P. Bustos, C. Berros, M.C. Diez, M.L. Mora, C. Gutierrez, Electrooxidation of 2,4-dichlorophenol and other polychlorinated phenols at glassy carbon electrode, *Electrochim. Acta* 47 (2002) 2399–2406.

[32] J.A. Richards, P.E. Whitson, D.H.J. Evans, Electrochemical oxidation of 2,4,6-tri-tert-buthylphenol, *J. Electroanal. Chem.* 63 (1975) 311–327.

[33] D.J. Walton, C.J. Campbell, P.G. Richards, J. Heptinstall, Electrooxidative nitration of phenols at copper electrodes, *Electrochim. Acta* 42 (1997) 3499–3507.

[34] S. Longchamp, N. Randriamabazaka, J.M. Nigretto, Electrochemical assay and properties of plasmin adsorbed onto a carbon paste electrode, *J. Electroanal. Chem.* 412 (1996) 31–37.

[35] M.Z. Wrona, G.J. Dryhurst, Oxidation chemistry of 5-hydroxytryptamine. 1. Mechanism and products formed at micromolar concentrations, *Org. Chem.* 52 (1987) 2817–2825.

[36] B.V. Sarada, T.N. Rao, D.A. Tryk, A. Fujishima, Electrochemical oxidation of histamine and serotonin at highly boron-doped diamond electrodes, *Anal. Chem.* 72 (2000) 1632–1638.

[37] S. Ito, T. Kato, K. Shinpo, K. Fujita, Oxidation of tyrosine residues in proteins by tyrosinase, *Biochem. J.* 222 (1984) 407–411.

[38] G.M. Robinson, E.I. Iwuocha, M.R. Smyth, Characterisation of electro-synthetic L-dopa-melanin films by electrochemical and spectroelectrochemical techniques, *Electrochim. Acta* 43 (1998) 3489–3496.